THE JOURNAL OF PHYSICAL CHEMISTRY B

Article

pubs.acs.org/JPCB

DNP-Enhanced MAS NMR of Bovine Serum Albumin Sediments and Solutions

Enrico Ravera,[†,∥] Björn Corzilius,[‡,§,∥] Vladimir K. Michaelis,[‡,∥] Claudio Luchinat,*[,†] Robert G. Griffin,*[,‡] and Ivano Bertini[†]

[†]Magnetic Resonance Center (CERM) and Department of Chemistry "Ugo Schiff", University of Florence, 50019 Sesto Fiorentino (FI), Italy

[‡]Francis Bitter Magnet Laboratory and Department of Chemistry, Massachusetts Institute of Technology, Cambridge, Massachusetts 02139, United States

ABSTRACT: Protein sedimentation sans cryoprotection is a new approach to magic angle spinning (MAS) and dynamic nuclear polarization (DNP) nuclear magnetic resonance (NMR) spectroscopy of proteins. It increases the sensitivity of the experiments by a factor of ∼4.5 in comparison to the conventional DNP sample preparation and circumvents intense background signals from the cryoprotectant. In this paper, we investigate sedimented samples and concentrated frozen solutions of natural abundance bovine serum albumin (BSA) in the absence of a glycerol-based cryoprotectant. We observe DNP signal enhancements of $\varepsilon \sim 66$ at 140 GHz in a BSA pellet sedimented from an aqueous solution containing the biradical polarizing agent TOTAPOL and compare this with samples prepared using the conventional protocol (i.e., dissolution of BSA in a glycerol/water cryoprotecting mixture). The dependence of DNP parameters on the radical concentration points to the presence of an interaction between TOTAPOL and BSA, so much so that a frozen solution sans cryoprotectant still gives $\varepsilon \sim 50$. We have studied the interaction of BSA with another biradical, SPIROPOL, that is more rigid than TOTAPOL and has been reported to give higher enhancements. SPIROPOL was also found to interact with BSA, and to give $\varepsilon \sim 26$ close to its maximum achievable concentration. Under the same conditions, TOTAPOL gives $\varepsilon \sim 31$, suggesting a lesser affinity of BSA for SPIROPOL with respect to TOTAPOL. Altogether, these results demonstrate that DNP is feasible in self-cryoprotecting samples.

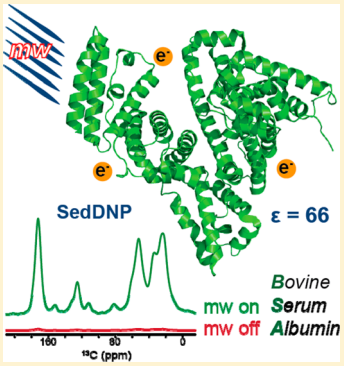

INTRODUCTION

Bovine serum albumin (BSA) is a highly soluble globular protein of 67 kDa molecular weight. BSA is known to stabilize biomolecules under otherwise denaturing conditions; for example, it has been shown to have cryoprotecting properties, reducing damage of enzymes during storage at low temperature.[1] Furthermore, with centrifugation, BSA forms a concentrated sediment (or pellet,[2−6] reported protein content values are about 600−700 mg/mL[2,4]), which is composed of a significant volume of protein which reduces the amount of free water within the sample.[4,7,8] This in turn is likely to limit the formation of neat ice crystals, at least in close proximity of the protein molecules (i.e., bound water is limited to the surface and pores of the protein, inhibiting degradation from freezing). The cryoprotective properties together with the tight packing of the protein molecules in a sediment layer might preserve the protein itself from cold denaturation processes.

Nuclear magnetic resonance (NMR) is an excellent spectroscopic technique to examine protein structure, function, and dynamics, especially in noncrystalline environments. In particular, NMR has the ability to locally probe the nuclei of interest providing both short- (<4 Å) and medium-range (4−7 Å) length scales. Unfortunately, because of the small nuclear Zeeman polarization, NMR is a low sensitivity technique, and therefore studies of low abundant nuclei (e.g., ^{13}C and ^{15}N) are often challenging. A highly successful method to increasing sensitivity is dynamic nuclear polarization (DNP), a concept initially proposed by Overhauser[9] and demonstrated soon thereafter by Carver and Slichter.[10] DNP relies on the transfer of electron polarization (typically from an organic based polarizing agent)[11−18] to neighboring nuclei, and for ^{1}H, a polarization enhancement of up to ∼660 can in principle be achieved.[19] In the 1990s, magic angle spinning (MAS) DNP utilizing gyrotrons as high power microwave sources[20−28] was introduced, and this led to widespread applications of DNP in MAS NMR studies,[29,30] especially of biological systems such as globular proteins, membrane proteins, nanocrystals, amyloid fibrils, and DNA[31−44,69] and more recently in materials science.[45−50]

For biological systems, the analyte is typically dispersed in a cryoprotecting solution containing the polarizing agent. Although homogeneous solutions of globular proteins can be investigated,[31] the ideal analyte forms a heterogeneous solution that is phase-separated from the cryoprotecting solvent/polarizing agent, for example, proteins embedded in a bilayer membrane,[32,36,37] amyloid fibrils,[33,34,51] or insoluble nanocryst-

Received: January 1, 2014
Revised: January 15, 2014
Published: January 24, 2014

   dx.doi.org/10.1021/jp500016f | J. Phys. Chem. B 2014, 118, 2957−2965

als.[33,51,52] The cryoprotecting properties of the glass-forming matrix prevent the phase separation of solvent and polarizing agent, and also prevent formation of grain boundaries due to crystallization upon freezing. The inhibition of crystallization allows for efficient dispersal of polarization from the bulk to the analyte. The sediment is to some extent separated from the bulk solvent; thus, an amorphous glass-like environment[53] may be formed at cryogenic temperatures. Recently, we demonstrated the possibility of studying NMR of sedimented solutes (SedNMR)[5,6,54−57] with DNP experiments. In particular, the sediment has proven as an ideal matrix for dispersing biradical polarizing agents and inhibiting crystallization, and therefore is an extremely suitable target for DNP, an approach which we termed SedDNP.[58]

In this study, we investigate BSA sedimented *ex situ*[6,53,54,59] from aqueous solutions by ultracentrifugation in order to further understand the requirements for sample preparation and cryoprotection. Examination of the DNP efficiency and radical-protein binding within the sedimented samples and solutions of varying protein concentration are also discussed. The results are of importance when a cryoprotectant is undesirable or the analyte concentration must be maximized.

MATERIALS AND METHODS

Sample Preparation. Bovine serum albumin (≥98%) was purchased from Sigma-Aldrich in lyophilized form and used without further purification. BSA protein was dissolved in either 90:10 (v/v) D_2O/H_2O or 60:30:10 (v/v/v) d_8-glycerol/D_2O/H_2O, and the appropriate biradical (2.5−10 mM, TOTAPOL[12] or SPIROPOL[11]) was added accordingly. Isotopically labeled solvents were purchased from Cambridge Isotope Laboratories (Andover, MA) and were used without further modification. Samples prepared with the 90:10 D_2O/H_2O water mixture were either used as such or sedimented for 24 h at 75 000 rpm using a Beckman L80K centrifuge equipped with a 100 Ti rotor. Further details are provided along with the results and figure captions, *vide infra*.

DNP NMR Spectroscopy. Dynamic nuclear polarization experiments were performed using a custom-built 212 MHz (5 T, ^{1}H) NMR spectrometer (courtesy of Dr. David Ruben, FBML-MIT), a 140 GHz gyrotron oscillator high power microwave source generating up to 14 W,[23] and a 4 mm triple resonance (^{1}H, ^{13}C, and ^{15}N) MAS DNP NMR probe. The probe uses an overmoded circular corrugated waveguide to efficiently couple microwaves to the sample and a sample eject mechanism allowing sample changing during cryogenic operation.[60] Experimental temperatures were maintained between 80 and 90 K by cooling the bearing and drive gas (N_2) using an external heat exchanger.[61] The magnetic field was set to the value yielding the maximum positive DNP enhancement for each biradical using a superconducting sweep coil generating a ±50 mT sweep width.

One-dimensional experiments involved destruction of thermal equilibrium polarization by a presaturation pulse train on both ^{1}H and ^{13}C, polarization of the ^{1}H matrix by continuous microwave irradiation during a variable polarization period, followed by ^{1}H−^{13}C ramped cross-polarization[62] (CP). ^{1}H and ^{13}C r.f. field strengths ($\gamma B_1/2\pi$) were adjusted to 100 kHz for each sample; the spin-lock field strength of ^{1}H was set to 100 kHz, while that of ^{13}C was optimized for efficient Hartmann−Hahn matching conditions at a MAS frequency of ($\omega_r/2\pi$) = 4.80 kHz. The CP contact time was found to be optimal at 1.2 ms. All spectra were acquired with TPPM[63] ^{1}H decoupling with $\gamma B_1/2\pi$ = 100 kHz. ^{1}H buildup times (T_B) were measured by varying the polarization period using an exponential increase from 0.1 up to 64 s; recycle delays where chosen to be 1.3 × T_B in order to maximize spectral S/N per unit of time. Depending on the sample concentration and sensitivity, between 8 and 90 000 transients were collected. Since the signal is averaged and not added, its intensity depends only on the Q of the r.f. circuitry and on the amount of sample in the rotor.

RESULTS AND DISCUSSION

BSA Sedimented DNP. Cryoprotection is often required when temperature cycling a protein below 273 K in order to avoid cold denaturation and to maintain the integrity of the protein structure at low temperatures (< −75 °C).[47,48] The addition of a glass-forming solvent, often glycerol, is used to inhibit bulk ice crystallization, enabling the formation of an amorphous solid that protects the protein, and disperses the polarizing agent if it is present. However, if, due to self-crowding, the tightly packed soluble protein forms a glassy state upon freezing of the water matrix, then the addition of a cryoprotectant is superfluous.[58] The feasibility of cryoprotectant-free DNP by sedimenting BSA was tested using a solution with an initial concentration of 100 mg/mL in 90/10 (v/v) D_2O/H_2O to which 5 mM TOTAPOL was added. Following centrifugation (75 000 rpm for 24 h), the sediment (∼50 μL) was packed into a sapphire rotor and inserted into the NMR probe, which had been precooled to cryogenic temperatures (between 85 and 90 K). Irradiation with 8 W of 140 GHz microwaves resulted in a 66-fold enhancement (ε) of the protein CPMAS NMR signal (Figure 1).

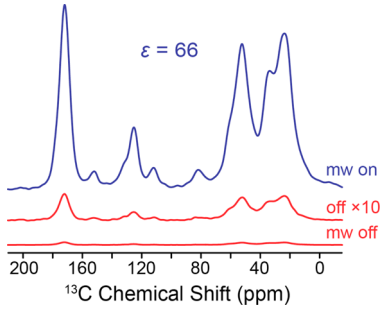

Figure 1. DNP-enhanced ("mw on", blue) and thermal equilibrium ("mw off", red) polarization ^{13}C-CPMAS spectrum of natural abundance BSA sedimented from a 100 mg/mL solution in 90/10 (v/v) D_2O/H_2O with 5 mM TOTAPOL. The thermal equilibrium spectrum has also been multiplied by a factor of 10 ("off × 10", red) for better comparison.

The magnitude of this enhancement is comparable to typical DNP experiments on proteins, where samples have been prepared by dissolving the protein in a glycerol/water mixture. However, the ^{1}H polarization buildup time constant of T_B = 1.8 s is short compared to a conventional approach. The rapid buildup of ^{1}H polarization is most likely caused by the high protein ^{1}H density in the sediment in combination with an increased biradical concentration due to potential protein−TOTAPOL interactions. In an earlier study, we have observed preferential enrichment of TOTAPOL in the sediment layer in SedDNP.[58] In order to further investigate this situation, the TOTAPOL concentration of the BSA solution was varied prior to sedimentation. Three samples

dx.doi.org/10.1021/jp500016f | J. Phys. Chem. B 2014, 118, 2957−2965

were prepared with 200 mg/mL BSA each and 2.5, 5, and 10 mM TOTAPOL concentration, respectively, and the results are shown in Figure 2. DNP enhancements increase, ε = 29, 48,

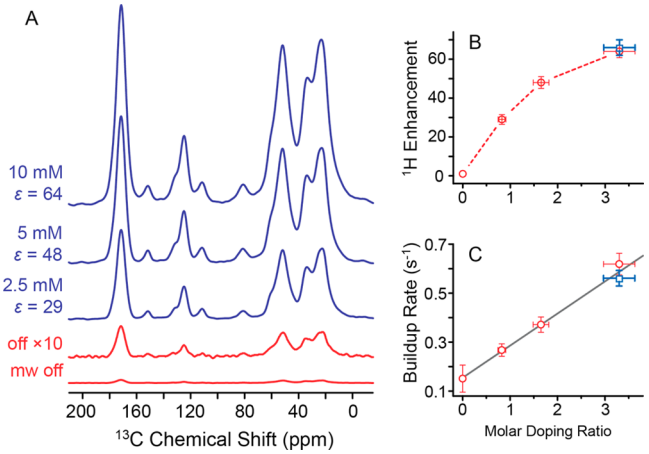

Figure 2. TOTAPOL concentration effect (2.5, 5, and 10 mM) on natural abundance BSA sedimented from 200 mg/mL (about 3 mM) protein solutions in 90/10 (v/v) D_2O/H_2O. (A) DNP enhancements with increasing TOTAPOL concentration (mM), (B) ^1H enhancement, and (C) polarization buildup rates as doping ratio (i.e., TOTAPOL/protein) increase. Open squares (blue) represent the sediment obtained from 100 mg/mL BSA solutions in 90/10 (v/v) D_2O/H_2O where 5 mM TOTAPOL was added (see Figure 1).

and 64, with increasing TOTAPOL concentration, while ^1H buildup times showed an inverse trend with T_B = 3.6, 2.6, and 1.6 s, respectively. In a control experiment, the spin–lattice relaxation time constant, T_1 = 6.3 s, was measured for a sample prepared in an identical manner sans TOTAPOL.

Interestingly, when comparing enhancements as well as buildup rates (i.e., T_B^{-1}) in Figure 2B and C, we observe very similar values for the sample sedimented from 100 mg/mL BSA doped with 5 mM TOTAPOL (blue, squares) and BSA sedimented from 200 mg/mL doped with 10 mM TOTAPOL (red circles). This suggests that it is not the absolute TOTAPOL concentration in the solution prior to centrifugation that is determining the TOTAPOL in the sediment but rather the TOTAPOL to protein concentration ratio (doping ratio) that is preserved during sedimentation. That would be the case if TOTAPOL were tightly or transiently binding to the protein, with the equilibrium much in favor of the protein–TOTAPOL complex in the solution. During centrifugation, TOTAPOL is then sedimented together with the protein (Figure 3A). A similar case has been observed during SedDNP for apoferritin and TOTAPOL.[58] Further parameters and details for all samples are provided below in Table 1. The last three columns of Table 1 assist in describing sensitivity by taking into account the final sedimented protein concentration (i.e., 600 mg/mL) and appropriate scaling for both DNP ^1H enhancement (c_{BSA}) and repetition rate ($T_B^{-1/2}$) and combining all parameters ($\varepsilon \times c_{BSA}/(T_B)^{1/2}$) to provide an overall enhancement factor. It is important to point out the enhancement previously recorded within sedimented apoferritin is most probably nonspecific due to the fact that the hydrophobic patches present on the protein surface are more concentrated in the sediment. This would provide a more suitable environment for the biradical TOTAPOL to partition within the sedimented protein layer with respect to the bulk

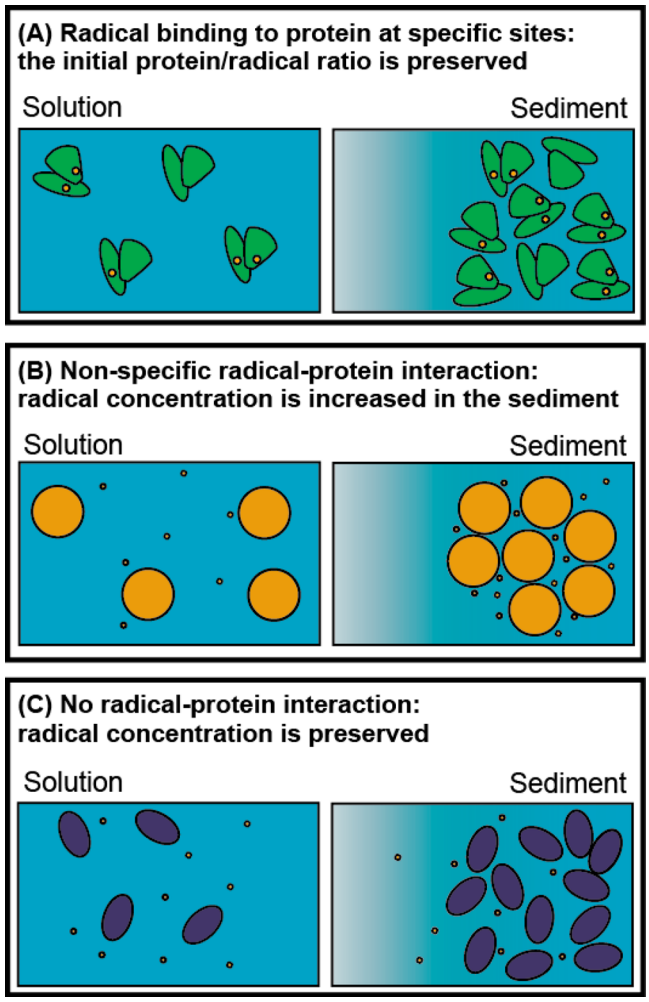

Figure 3. Effect of three different protein–radical interaction modes on the radical distribution in sedimented proteins. Part A depicts the situation described in the present work: the radical binds to the protein and thus the radical/protein ratio is preserved when moving from solution to the sediment. Part B represents the situation previously described,[58] where the radical is partitioned in the more hydrophilic sediment. Part C shows a theoretical case in which the protein is sedimented but the radical preserves the same distribution throughout the sample.

solution (Figure 3B). Figure 3C represents a situation that has not yet been encountered where the protein does not interact with the radical. In this case, it is expected that the concentration of the radical will be uniform throughout the sample, regardless of the gradient formed by the protein, and this situation is not different from the radical distribution observed in the usual DNP sample (i.e., d_8-glycerol/D_2O/H_2O).

Direct binding between BSA and TOTAPOL is not unexpected. BSA contains two hydrophobic binding sites that could provide a preferential environment for the partially hydrophobic TOTAPOL. Furthermore, TOTAPOL possesses a relatively flexible structure, allowing it to adopt a conformation suitable for binding. The combination of amphiphilicity and flexibility could further improve TOTAPOL's tendency to interact with the protein, allowing a molar ratio between bound TOTAPOL and BSA larger than 2. At the same time, it is important to emphasize that radical binding to the protein is not an intrinsic feature of MAS DNP but rather an intrinsic

dx.doi.org/10.1021/jp500016f | J. Phys. Chem. B 2014, 118, 2957–2965

Table 1. BSA Sample Conditions and DNP NMR Results for a Series of BSA/TOTAPOL Sedimented Mixtures (SedDNP)

c_{BSA} [a] (mM)	$c_{TOTAPOL}$ [a] (mM)	$c_{TOTAPOL}/c_{BSA}$ [a] (doping ratio)	ε	T_B (s)	$\varepsilon \times c_{BSA}$ [b] (mM)	$\varepsilon/(T_B)^{1/2}$ ($s^{-1/2}$)	$\varepsilon \times c_{BSA}/(T_B)^{1/2}$ [b] (mM $s^{-1/2}$)
3.03 (200 mg/mL)	0.0	0.00		6.3	9.1	0.4	3.6
3.03 (200 mg/mL)	2.5	0.83	29	3.6	263.6	15.2	138.1
3.03 (200 mg/mL)	5.0	1.65	48	2.6	436.3	29.5	268.3
3.03 (200 mg/mL)	10.0	3.29	64	1.6	581.8	50.6	460.1
1.52 (100 mg/mL)	5.0	3.29	66	1.8	601.9	49.2	448.6

[a]Initial concentration before sedimentation. [b]The BSA concentration in the sediment is assumed to be 600 mg/mL (i.e., a factor of 3−6 times larger than presedimented starting material).[2]

feature of the chemistry of the biomolecule under investigation, in this case a protein that is able to tightly bind a number of nonspecific partners.[64]

BSA Concentrated Solution DNP. In contrast to other studies performed on non-cryoprotected samples,[58] all BSA solutions maintained a DNP-supporting state even without sedimentation. Figure 4 shows DNP-enhanced spectra obtained from 90/10 (v/v of D_2O/H_2O) solutions containing between 50 and 400 mg/mL BSA doped with 5 mM TOTAPOL each. The enhancement reached a maximum of ε = 50 for 100 mg/mL BSA, while the maximum signal intensity was obtained with the highest concentrated sample of 400 mg/mL, where an enhancement factor of 31 was observed. A maximum enhancement was achieved for a TOTAPOL/BSA doping ratio between 1.5 and 3 (100 and 200 mg/mL), as shown in Figure 4B. The reduction of enhancement with increases in the doping ratio is expected and has been seen in other studies.[65] It is not an effect of different binding behavior but rather the elevated radical concentration accelerating the inherent longitudinal relaxation due to increasing paramagnetic broadening, which causes a reduction in the observed enhancements. The polarization buildup rate increased almost linearly with increasing doping ratio (Figure 4C). All data are compiled in Table 2, including the appropriate scaling factors for sensitivity as a function of BSA concentration (c_{BSA}), buildup time ($T_B^{-1/2}$), and overall sensitivity ($\varepsilon \times c_{BSA}/(T_B)^{1/2}$). These findings clearly indicate a strong correlation between the doping ratio and DNP parameters, whereas in other studies using a glycerol/water mixture the absolute TOTAPOL concentration determines enhancement and buildup time constant.[65] In the latter case, the polarization of the analyte occurs mainly due to spin-diffusion through the bulk protons; the analyte concentration does not significantly influence DNP, indicating that no binding is occurring between the radical and the analyte. Conversely, in the present study, we find that binding occurs between the radical and the analyte, and seems to prevent radical segregation upon freezing of the bulk water.

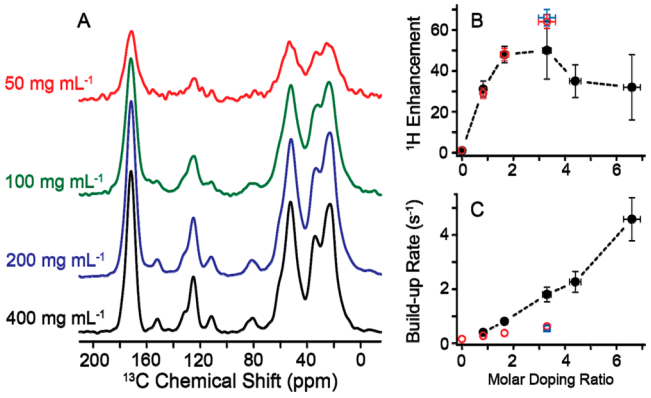

Figure 4. BSA concentration effects in 90/10 (v/v) D_2O/H_2O solutions containing 5 mM TOTAPOL (closed circles, black). Overall DNP-enhanced sensitivity with increasing protein concentration (A), ^1H enhancement (B), and polarization buildup rates as doping ratio (i.e., $c_{TOTAPOL}/c_{BSA}$) increases (C). Open circles (red) represent data points obtained from 200 mg/mL BSA sedimented samples (see Figure 2). Open squares (blue) represent the sediment obtained from 100 mg/mL BSA solutions in 90/10 (v/v) D_2O/H_2O where 5 mM TOTAPOL was added (see Figure 1).

Sample Preparation Approaches. The efficiency of preparation sans glass-forming agent was compared with two common DNP sample preparations: (i) dissolution of the protein in a 60/30/10 (v/v/v) mixture of d_8-glycerol/D_2O/H_2O to which TOTAPOL is added and (ii) direct addition of d_8-glycerol to the BSA sediment. Figure 5A shows the DNP-enhanced NMR spectrum of 160 mg/mL BSA in 60/30/10 (v/v/v) d_8-$^{12}C_3$-glycerol/D_2O/H_2O (isotopically depleted glycerol containing 0.05% ^{13}C) doped with 5 mM TOTAPOL. The maximum concentration achievable by first dissolving BSA in water (400 mg/mL) and then mixing the solution with the appropriate amount of glycerol was 160 mg/mL. Figure 5B shows spectra obtained by sedimenting BSA from a 200 mg/mL solution in 90/10 (v/v) D_2O/H_2O, where an equal volume of d_8-$^{12}C_3$-glycerol (0.05% ^{13}C) was added to the sediment after removal of the supernatant solution. Figure 5C shows data obtained from a sample prepared identically but using d_8-glycerol with natural abundance carbon (1.1% ^{13}C). DNP enhancements of 78 and T_B = 3.4 s were observed for the dissolved BSA sample, while for the cryoprotected sediments ε = 56 and 59 with T_B = 5.3 and 5.1 s were obtained,

Table 2. BSA Sample Conditions and DNP NMR Results for a Series of BSA/TOTAPOL Solutions (Concentrated Solution DNP)

c_{BSA} (mM)	$c_{TOTAPOL}/c_{BSA}$ (doping ratio)	ε	T_B (s)	$\varepsilon \times c_{BSA}$ (mM)	$\varepsilon/(T_B)^{1/2}$ ($s^{-0.5}$)	$\varepsilon \times c_{BSA}/(T_B)^{1/2}$ (mM $s^{-0.5}$)
0.75 (50 mg/mL)	6.67	32	0.22	24.2	68.5	51.9
1.14 (75 mg/mL)	4.39	35	0.44	39.8	52.7	59.9
1.52 (100 mg/mL)	3.29	50	0.55	75.8	67.2	101.8
3.03 (200 mg/mL)	1.65	48	1.23	145.4	43.2	131.0
6.06 (400 mg/mL)	0.83	31	2.47	187.9	19.7	119.6

dx.doi.org/10.1021/jp500016f | J. Phys. Chem. B 2014, 118, 2957−2965

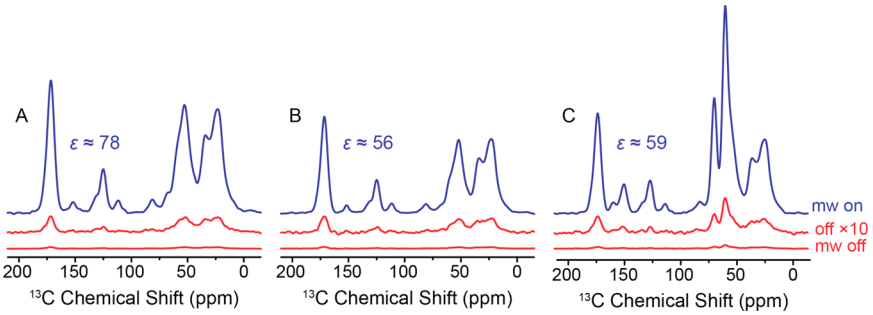

Figure 5. Effect of common cryoprotecting methods on DNP-enhanced ^{13}C-CPMAS spectra of natural abundance BSA. d_8-$^{12}C_3$-glycerol (0.05% ^{13}C) protected using 60/30/10 (v/v/v) of glycerol/D_2O/H_2O (A) or sedimented in a 90/10 (v/v) D_2O/H_2O matrix and mixed with an equal volume of d_8-$^{12}C_3$-glycerol (0.05% ^{13}C) (B) or d_8-glycerol (1.1% ^{13}C) (C) at constant biradical concentration. Please note the conditions for part C are identical to those in part B except d_8-glycerol with natural abundance in carbon (1.1% ^{13}C) has been used.

respectively. The small difference between the two latter samples lies well within the experimental uncertainty.

Figure 5C illustrates the problem of significant ^{13}C background from residual ^{13}C-glycerol overlapping with the Cα spectral region in this case of the natural abundance BSA. This background can be circumvented either by utilizing isotopically depleted solvent or by application of this novel method of cryoprotectant-free DNP.

Protein/Radical Interactions. Figure 6 summarizes the effect of specific protein−radical binding on the DNP

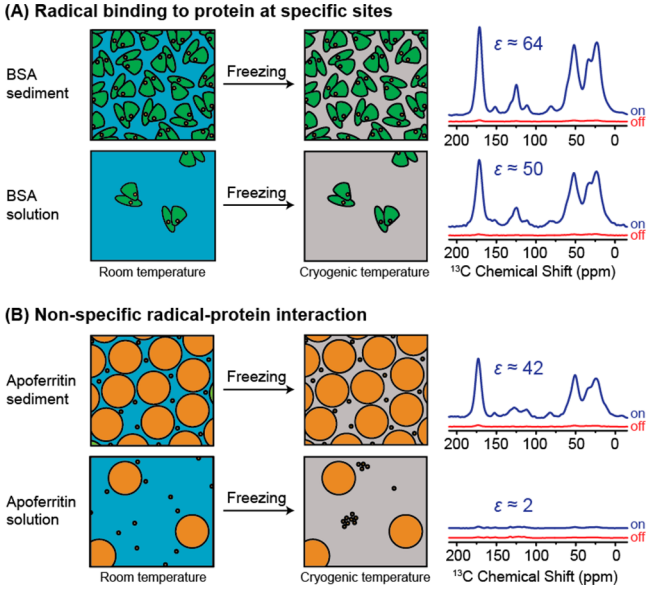

Figure 6. Comparison between the present model of tight radical protein binding (top panel, A) and the segregation model previously discussed for the case of apoferritin[58] (bottom panel, B).

performance under the distinct conditions of sediment and highly concentrated solutions. When the binding is strong as is the case in the study at hand, the radical that is bound in solution remains with the protein also when the solution is frozen. On the contrary, if the interaction is weak, the radical tends to partition into the more hydrophobic sediment rather in the aqueous solution, but when the sediment is not present the radical will tend to segregate. The latter case has been observed in a previous article by the same authors on the protein complex apoferritin.[58]

The data at hand clearly raises the question of the sample preparation method that optimizes the DNP-enhanced NMR sensitivity. This sensitivity is not only determined by DNP enhancement factors but also depends strongly on the optimal recycle delay between acquisitions and therefore on the buildup time constant. Another simpler factor determining sensitivity is the analyte concentration. Generally, a shorter recycle delay allows for faster acquisition of the spectra; however, in many cases, the minimum recycle delay is determined by instrumental limitations. Although sample heating is of minor concern during DNP experiments due to active sample cooling and low dielectric properties of the frozen sample, high-power decoupling of protons results in a significant rf duty cycle at short recycle delays. In cases where the recycle delay is instrumentally limited, a quantitative assessment of sensitivity cannot be straightforwardly given. Several measures of sensitivity are given in Tables 1 and 2, including effects from DNP enhancement (ε), the size of the recycle delay ($T_B^{-1/2}$), and analyte concentration (c_{BSA}). In Figure 7, the overall DNP-

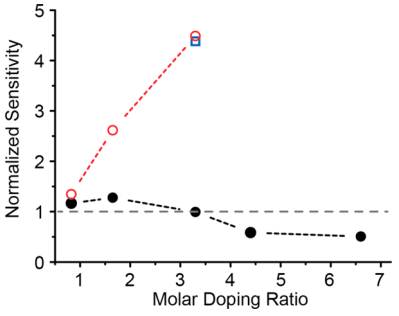

Figure 7. DNP-enhanced NMR sensitivity of BSA samples with increased TOTAPOL to protein doping ratio. BSA solutions (filled circles, black), sedimented samples from 200 mg/mL (open circles, red), and the sedimented sample from 100 mg/mL solution (open square, blue) are shown in comparison with the sensitivity obtained from 160 mg/mL BSA in 60/30/10 (v/v/v) d_8-glycerol/D_2O/H_2O with 5 mM TOTAPOL (dashed line, gray).

enhanced NMR sensitivity ($\varepsilon \times c_{BSA}/(T_B)^{1/2}$) is shown for sediments (Table 1) and concentrated solutions (Table 2) of BSA in 90:10 (D_2O/H_2O). Although the sediment concentration of BSA is not known exactly, we may assume a concentration of 600 mg/mL, based on literature values.[53] Clearly, the sedimented BSA yields a larger sensitivity than the solutions at any given doping ratio investigated in this study due to the large analyte concentration. More interestingly,

dx.doi.org/10.1021/jp500016f | J. Phys. Chem. B 2014, 118, 2957−2965

solutions with large BSA concentrations and BSA sediments yield sensitivities superior to those obtained with a glycerol/water solution; in particular, a sensitivity gain of almost 5-fold can be obtained with the sediment.

The potential for signal quenching induced by strong paramagnetic interactions is always of concern, although challenging to measure accurately due to variable issues. To account for paramagnetic quenching effects within the sedimented samples, four ^{13}C-CPMAS experiments were acquired under identical conditions (i.e., sample volume (50 ± 5 μL), BSA concentration (200 mg/mL), temperature, recycle delay (1.3 × T_B), spectrometer parameters (e.g., gain, CP parameters, coadded transients, etc.), and performing all experiments without microwaves). Even with this careful attention to detail, we expect our uncertainty in these measurements to be approximately 10% of the observed signal intensity. Using the off signal from the nondoped sample scaled to 1, we ascertain that doping ratios <1 are well within experimental error and minimize quenching effects; heading toward a doping ratio of 3, a loss of 40 ± 10% is observed (Figure 8). These interactions have been recently studied

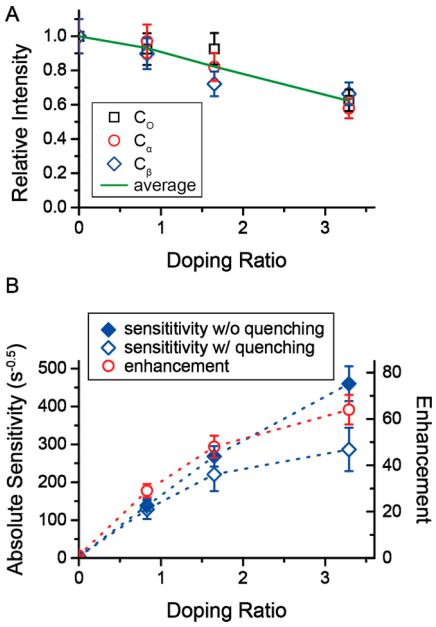

Figure 8. Paramagnetic signal quenching effects on the 200 mg/mL sedimented BSA samples. (A) Paramagnetic signal quenching for the carbonyl (C_O) and aliphatic (C_α and C_β) regions, determined from a prepared sample without radical (NB: off-signals were compared for four sedimented BSA samples ranging from 0 to 3.29 doping ratio). (B) DNP-enhanced NMR sensitivity of BSA samples with increased TOTAPOL to protein doping ratio, ^{1}H DNP enhancement (open circles, red), absolute sensitivity with paramagnetic quenching (open diamonds, blue), and absolute sensitivity without paramagnetic quenching (closed diamonds, blue).

extensively by Corzilius et al.,[66] whereby a loss in signal intensity occurs while under magic-angle spinning conditions but does not occur for nonspinning samples. These losses in signal have been seen for both the narrow-line radical, trityl (~35%), and the wide-line nitroxide biradical, TOTAPOL (~45%), in agreement with our study on sedimented BSA. Although the paramagnet induces some quenching of the ^{13}C signal intensity, Figure 8A illustrates the significant gain in overall sensitivity when the overall DNP-enhanced sensitivity ($E = \varepsilon \times c_{BSA}/(T_B)^{1/2}$) is taken and multiplied by paramagnetic quenching observed from the off spectrum (Figure 8B). This treatment was not applied to the DNP-enhanced BSA concentrated solutions due to the drastic differences in protein concentrations (i.e., 50 mg/mL vs 400 mg/mL could lead to significant scaling issues of the off-signal) and difficulties in maintaining identical probe efficiency due to the drastically different physical (i.e., dielectric) properties of a low (e.g., <100 mg/mL) versus a high (>200 mg/mL) viscosity sample.

Direct binding interactions between TOTAPOL and BSA potentially raise concerns about paramagnetic interactions and resonance broadening of protein NMR signals. Quantifying paramagnetic broadening was attempted by analyzing the line width of the carbonyl resonance. Although the line shape represents the envelope of all individual carbonyl resonances (~582) of the protein and is therefore due mainly to inhomogeneous effects, it serves as an acceptable first approximation to measure for possible homogeneous broadening. Results are shown in Figure 9. The full width at half-

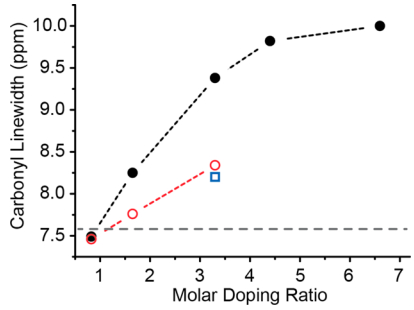

Figure 9. Effect of increasing doping ratio on paramagnetic broadening of BSA. BSA solutions (filled circles, black), sedimented samples from 200 mg/mL (open circles, red), sedimented sample from 100 mg/mL solution (open square, blue), and the 160 mg/mL BSA in 60/30/10 (v/v/v) d_8-glycerol/D_2O/H_2O with 5 mM TOTAPOL (dashed line, gray).

maximum (fwhm) is found to vary between ~7.5 and 10 ppm. Interestingly, both the sedimented BSA sample as well as the solution with the lowest doping ratio of ~0.83 ($c_{TOTAPOL}/c_{BSA}$) show line widths slightly below the line width found for the BSA solution in glycerol/water (7.6 ppm). On the basis of these data, we conclude that line broadening is of little or no concern in comparison to the "standard" DNP sample preparation, as long as the doping ratio is kept low. As such, a three-way balance is achieved in order to optimize radical concentration for buildup times, enhancement, and resolution at cryogenic temperatures. The study of natural abundance BSA limits our ability to probe specific sites in order to ascertain signal quenching or broadening in the hydrophobic region of the protein are not possible at this time. By applying selective labeling protocols and moving toward high-field DNP NMR spectrometers (i.e., 600/395,[67] 700/460,[26] and 800/527[68] MHz/GHz), it will be possible to achieve further resolution and further details regarding protein−radical interactions.

The clear interaction between BSA and TOTAPOL prompted an evaluation of the binding behavior in the presence of a different radical, SPIROPOL (Figure 10), that has been shown to yield ~20% larger enhancement for model systems as compared to TOTAPOL while still being soluble in glycerol/water mixtures. However, the solubility in pure water is limited to 3 mM.[11] Like TOTAPOL, SPIROPOL is a bis-nitroxide-

dx.doi.org/10.1021/jp500016f | J. Phys. Chem. B 2014, 118, 2957−2965

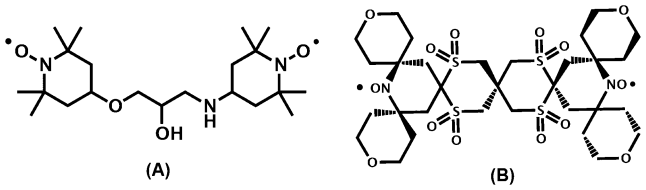

Figure 10. Chemical structures of the biradicals TOTAPOL (A) and SPIROPOL (B). NB: For simplicity SPIROPOL is depicted above with sulfonyl groups, these functional groups are in fact a mixture of sulfonyls, sulfoxides and thioethers as presented in Kiesewetter et al.[11]

based radical but it is bulkier and less flexible, and thus might show different binding affinity toward BSA (Figure 10). In a control experiment, SPIROPOL did yield a larger enhancement in a 5 mM 60/30/10 d_8-glycerol/D_2O/H_2O solution containing 160 mg/mL BSA. In particular, ε = 89 is about 14% larger than ε = 78 found for TOTAPOL under otherwise identical conditions. However, when comparing the DNP behavior in a 90/10 (v/v D_2O/H_2O) solution containing 400 mg/mL BSA, the enhancement obtained with 2.5 mM SPIROPOL (ε = 26) was lower than that measured using the same concentration of TOTAPOL (ε = 31). The reason for this is not yet clear. As already mentioned, the differences in flexibility and hydrophobicity might lead to different binding behavior. At the same time, SPIROPOL is used at the upper limit of its solubility in water and might undergo a more pronounced phase separation within the bulk water during freezing. On the basis of these results, we suspect that TOTAPOL may have a higher affinity for BSA than SPIROPOL. This leads to an improved ^{1}H DNP enhancement of the former within the concentrated solution, whereas SPIROPOL is more effective in the traditional glassing matrix (glycerol/water).

SUMMARY

Using a model globular protein, BSA, a high-throughput method using sedimentation preparation has been demonstrated, which reduces the need for a cryoprotecting matrix in DNP experiments. The sedimentation approach provides efficient DNP enhancements while circumventing unwanted background signals, which can affect systems in natural abundance, limited sample volumes, or sparsely labeled large biological solids. Utilizing various sample preparation approaches and radical concentrations, we have proposed three radical/protein interaction models, which can affect the SedDNP approach. BSA/TOTAPOL binding was determined to be site-specific, whereas our previous study on apoferritin/TOTAPOL exhibited nonspecific binding, thus requiring *in situ* sedimentation for effective DNP. Substituting the type of polarizing agent (i.e., SPIROPOL vs TOTAPOL) may allow adjustment of radical/protein interaction to maintain effective sensitivity gain and minimize broadening effects on NMR spectra. We have shown the SedDNP method provides a facet for high sample throughput in order to achieve significant gains in sensitivity, while maintaining clean, background-free ^{13}C spectra. With further investigations of the sedimentation process for DNP NMR, this approach may be applied to selectively labeled biological systems for improved access to determination of structure and function.

AUTHOR INFORMATION

Corresponding Authors

*E-mail: luchinat@cerm.unifi.it. Phone: +39-055-457-4296.
*E-mail: rgg@mit.edu. Phone: 617-253-5597.

Present Address

[§]Institute for Physical and Theoretical Chemistry, Insitute for Biophysical Chemistry, and Center for Biomolecular Magnetic Resonance, Goethe University Frankfurt, Max-von-Laue-Str. 9, 60438 Frankfurt am Main, Germany.

Author Contributions

[‖]These authors contributed equally to this work.

Notes

The authors declare no competing financial interest.

ACKNOWLEDGMENTS

The authors dedicate this article to Professor Ivano Bertini, who passed away during the course of this research (July 7th, 2012). The authors would like to thank Ta-Chung Ong and Jeffrey Bryant for useful discussions during the course of this research. Prof. Giacomo Parigi (CERM, University of Florence) is acknowledged for several helpful discussions and a critical review of the manuscript. This work was supported by the EC contracts East-NMR n. 228461 and Bio-NMR n. 261863 (WP21), COST action TD1103, INSTRUCT (European FP7 e-Infrastructure grant, contract no. 211252, http://www.instruct-fp7.eu/), the MIUR PRIN (2009FAKHZT_001), Ente Cassa di risparmio di Firenze (I.B. and C.L.), and the National Institute of Health through grants EB-002804, EB-003151, and EB-002026 (R.G.G.). V.K.M. is grateful to the Natural Sciences and Engineering Research Council (NSERC) of Canada for a postdoctoral fellowship. B.C. was partially supported by the Deutsche Forschungsgemeinschaft through research fellowship CO 802/1-1.

REFERENCES

(1) Tamiya, T.; Okahashi, N.; Sakuma, R.; Aoyama, T.; Akahane, T.; Matsumoto, J. J. Freeze Denaturation of Enzymes and its Prevention with Additives. *Cryobiology* **1985**, *22* (5), 446−456.
(2) Lundh, S. Concentrated Protein Solutions in the Analytical Ultra-Centrifuge. *J. Polym. Sci., Part B: Polym. Phys.* **1980**, *18* (9), 1963−1978.
(3) Minton, A. P.; Lewis, M. S. Self-Association in Highly Concentrated-Solutions of Myoglobin - a Novel Analysis of Sedimentation Equilibrium of Highly Nonideal Solutions. *Biophys. Chem.* **1981**, *14* (4), 317−324.
(4) Lundh, S. Ultracentrifugation of Concentrated Bio-Polymer Solutions and Effect of Ascorbate. *Arch. Biochem. Biophys.* **1985**, *241* (1), 265−274.
(5) Bertini, I.; Luchinat, C.; Parigi, G.; Ravera, E.; Reif, B.; Turano, P. Solid-State NMR of Proteins Sedimented by Ultracentrifugation. *Proc. Natl. Acad. Sci. U.S.A.* **2011**, *108* (26), 10396−10399.
(6) Bertini, I.; Engelke, F.; Luchinat, C.; Parigi, G.; Ravera, E.; Rosa, C.; Turano, P. NMR Properties of Sedimented Solutes. *Phys. Chem. Chem. Phys.* **2012**, *14* (2), 439−447.
(7) Zimmerman, S. B.; Minton, A. P. Macromolecular Crowding - Biochemical, Biophysical, and Physiological Consequences. *Annu. Rev. Biophys. Biomol. Struct.* **1993**, *22*, 27−65.
(8) Luchinat, C.; Parigi, G.; Ravera, E. Water and Protein Dynamics in Sedimented Systems: A Relaxometric Investigation. *ChemPhysChem* **2013**, *14* (13), 3156−3161.
(9) Overhauser, A. W. Polarization of Nuclei in Metals. *Phys. Rev.* **1953**, *92* (2), 411−415.
(10) Carver, T. R.; Slichter, C. P. Polarization of Nuclear Spins in Metals. *Phys. Rev.* **1953**, *92* (1), 212−213.

(11) Kiesewetter, M. K.; Corzilius, B.; Smith, A. A.; Griffin, R. G.; Swager, T. M. Dynamic Nuclear Polarization with a Water-Soluble Rigid Biradical. *J. Am. Chem. Soc.* **2012**, *134* (10), 4537−4540.
(12) Song, C.; Hu, K.-N.; Joo, C.-G.; Swager, T. M.; Griffin, R. G. TOTAPOL: A Biradical Polarizing Agent for Dynamic Nuclear Polarization Experiments in Aqueous Media. *J. Am. Chem. Soc.* **2006**, *128* (35), 11385−11390.
(13) Ysacco, C.; Karoui, H.; Casano, G.; Moigne, F.; Combes, S.; Rockenbauer, A.; Rosay, M.; Maas, W.; Ouari, O.; Tordo, P. Dinitroxides for Solid State Dynamic Nuclear Polarization. *Appl. Magn. Reson.* **2012**, *43* (1−2), 251−261.
(14) Zagdoun, A.; Casano, G.; Ouari, O.; Lapadula, G.; Rossini, A. J.; Lelli, M.; Baffert, M.; Gajan, D.; Veyre, L.; Maas, W. E.; et al. A Slowly Relaxing Rigid Biradical for Efficient Dynamic Nuclear Polarization Surface-Enhanced NMR Spectroscopy: Expeditious Characterization of Functional Group Manipulation in Hybrid Materials. *J. Am. Chem. Soc.* **2011**, *134* (4), 2284−2291.
(15) Haze, O.; Corzilius, B.; Smith, A. A.; Griffin, R. G.; Swager, T. M. Water-Soluble Organic Radicals as Polarizing Agents for High Field Dynamic Nuclear Polarization. *J. Am. Chem. Soc.* **2012**, *134* (35), 14287−14290.
(16) Dane, E. L.; Corzilius, B.; Rizzato, E.; Stocker, P.; Maly, T.; Smith, A. A.; Griffin, R. G.; Ouari, O.; Tordo, P.; Swager, T. M. Rigid Orthogonal Bis-Tempo Biradicals with Improved Solubility for Dynamic Nuclear Polarization. *J. Org. Chem.* **2012**, *77* (4), 1789−1797.
(17) Dane, E. L.; Maly, T.; Debelouchina, G. T.; Griffin, R. G.; Swager, T. M. Synthesis of a BDPA-Tempo Biradical. *Org. Lett.* **2009**, *11* (9), 1871−1874.
(18) Thurber, K. R.; Yau, W.-M.; Tycko, R. Low-Temperature Dynamic Nuclear Polarization at 9.4 T with a 30 mW Microwave Source. *J. Magn. Reson.* **2010**, *204* (2), 303−313.
(19) Abragam, A.; Goldman, M. Principles of Dynamic Nuclear Polarization. *Rep. Prog. Phys.* **1978**, *41* (3), 395−467.
(20) Bajaj, V. S.; Farrar, C. T.; Hornstein, M. K.; Mastovsky, I.; Vieregg, J.; Bryant, J.; Elena, B.; Kreischer, K. E.; Temkin, R. J.; Griffin, R. G. Dynamic Nuclear Polarization at 9 T using a Novel 250 GHz Gyrotron Microwave Source. *J. Magn. Reson.* **2003**, *160* (2), 85−90.
(21) Bajaj, V. S.; Hornstein, M. K.; Kreischer, K. E.; Sirigiri, J. R.; Woskov, P. P.; Mak-Jurkauskas, M. L.; Herzfeld, J.; Temkin, R. J.; Griffin, R. G. 250 GHz CW Gyrotron Oscillator for Dynamic Nuclear Polarization in Biological Solid State NMR. *J. Magn. Reson.* **2007**, *189* (2), 251−279.
(22) Becerra, L. R.; Gerfen, G. J.; Bellew, B. F.; Bryant, J. A.; Hall, D. A.; Inati, S. J.; Weber, R. T.; Un, S.; Prisner, T. F.; McDermott, A. E.; et al. A Spectrometer for Dynamic Nuclear Polarization and Electron Paramagnetic Resonance at High-Frequencies. *J. Magn. Reson., Ser. A* **1995**, *117* (1), 28−40.
(23) Becerra, L. R.; Gerfen, G. J.; Temkin, R. J.; Singel, D. J.; Griffin, R. G. Dynamic Nuclear Polarization with a Cyclotron Resonance Maser at 5 T. *Phys. Rev. Lett.* **1993**, *71* (21), 3561−3564.
(24) Rosay, M.; Tometich, L.; Pawsey, S.; Bader, R.; Schauwecker, R.; Blank, M.; Borchard, P. M.; Cauffman, S. R.; Felch, K. L.; Weber, R. T.; et al. Solid-State Dynamic Nuclear Polarization at 263 GHz: Spectrometer Design and Experimental Results. *Phys. Chem. Chem. Phys.* **2010**, *12* (22), 5850−5860.
(25) Gerfen, G. J.; Becerra, L. R.; Hall, D. A.; Griffin, R. G.; Temkin, R. J.; Singel, D. J. High Frequency (140 GHz) Dynamic Nuclear Polarization: Polarization Transfer to a Solute in Frozen Aqueous Solution. *J. Chem. Phys.* **1995**, *102* (24), 9494−7.
(26) Barnes, A. B.; Markhasin, E.; Daviso, E.; Michaelis, V. K.; Nanni, E. A.; Jawla, S. K.; Mena, E. L.; DeRocher, R.; Thakkar, A.; Woskov, P. P.; et al. Dynamic Nuclear Polarization at 700 MHz/460 GHz. *J. Magn. Reson.* **2012**, *224*, 1−7.
(27) Matsuki, Y.; Ueda, K.; Idehara, T.; Ikeda, R.; Ogawa, I.; Nakamura, S.; Toda, M.; Anai, T.; Fujiwara, T. Helium-Cooling and -Spinning Dynamic Nuclear Polarization for Sensitivity-Enhanced Solid-State NMR at 14 T and 30 K. *J. Magn. Reson.* **2012**, *225* (0), 1−9.
(28) Matsuki, Y.; Takahashi, H.; Ueda, K.; Idehara, T.; Ogawa, I.; Toda, M.; Akutsu, H.; Fujiwara, T. Dynamic Nuclear Polarization Experiments at 14.1 T for Solid-State NMR. *Phys. Chem. Chem. Phys.* **2010**, *12* (22), 5799−5803.
(29) Corzilius, B.; Smith, A. A.; Barnes, A. B.; Luchinat, C.; Bertini, I.; Griffin, R. G. High-Field Dynamic Nuclear Polarization with High-Spin Transition Metal Ions. *J. Am. Chem. Soc.* **2011**, *133* (15), 5648−5651.
(30) Michaelis, V. K.; Markhasin, E.; Daviso, E.; Herzfeld, J.; Griffin, R. G. Dynamic Nuclear Polarization of Oxygen-17. *J. Phys. Chem. Lett.* **2012**, *3*, 2030−2034.
(31) Akbey, U.; Franks, W. T.; Linden, A.; Lange, S.; Griffin, R. G.; van Rossum, B. J.; Oschkinat, H. Dynamic Nuclear Polarization of Deuterated Proteins. *Angew. Chem., Int. Ed.* **2010**, *49* (42), 7803−7806.
(32) Bajaj, V. S.; Mak-Jurkauskas, M. L.; Belenky, M.; Herzfeld, J.; Griffin, R. G. Functional and Shunt States of Bacteriorhodopsin Resolved by 250 GHz Dynamic Nuclear Polarization-Enhanced Solid-State NMR. *Proc. Natl. Acad. Sci. U.S.A.* **2009**, *106* (23), 9244−9249.
(33) Debelouchina, G. T.; Bayro, M. J.; van der Wel, P. C. A.; Caporini, M. A.; Barnes, A. B.; Rosay, M.; Maas, W. E.; Griffin, R. G. Dynamic Nuclear Polarization-Enhanced Solid-State NMR Spectroscopy of GNNQQNY Nanocrystals and Amyloid Fibrils. *Phys. Chem. Chem. Phys.* **2010**, *12* (22), 5911−5919.
(34) Bayro, M. J.; Debelouchina, G. T.; Eddy, M. T.; Birkett, N. R.; MacPhee, C. E.; Rosay, M.; Maas, W. E.; Dobson, C. M.; Griffin, R. G. Intermolecular Structure Determination of Amyloid Fibrils with Magic-Angle Spinning and Dynamic Nuclear Polarization NMR. *J. Am. Chem. Soc.* **2011**, *133* (35), 13967−13974.
(35) Sergeyev, I. V.; Day, L. A.; Goldbourt, A.; McDermott, A. E. Chemical Shifts for the Unusual DNA Structure in Pf1 Bacteriophage from Dynamic-Nuclear-Polarization-Enhanced Solid-State NMR Spectroscopy. *J. Am. Chem. Soc.* **2012**, *133* (50), 20208−20217.
(36) Linden, A. H.; Lange, S.; Franks, W. T.; Akbey, Ü.; Specker, E.; van Rossum, B.-J.; Oschkinat, H. Neurotoxin II Bound to Acetylcholine Receptors in Native Membranes Studied by Dynamic Nuclear Polarization NMR. *J. Am. Chem. Soc.* **2011**, *133* (48), 19266−19269.
(37) Mak-Jurkauskas, M. L.; Bajaj, V. S.; Hornstein, M. K.; Belenky, M.; Griffin, R. G.; Herzfeld, J. Energy Transformations Early in the Bacteriorhodopsin Photocycle Revealed by DNP-Enhanced Solid-State NMR. *Proc. Natl. Acad. Sci. U.S.A.* **2008**, *105* (3), 883−888.
(38) Jacso, T.; Franks, W. T.; Rose, H.; Fink, U.; Broecker, J.; Keller, S.; Oschkinat, H.; Reif, B. Characterization of Membrane Proteins in Isolated Native Cellular Membranes by Dynamic Nuclear Polarization Solid-State NMR Spectroscopy without Purification and Reconstitution. *Angew. Chem., Int. Ed.* **2012**, *51* (2), 432−435.
(39) Reggie, L.; Lopez, J. J.; Collinson, I.; Glaubitz, C.; Lorch, M. Dynamic Nuclear Polarization-Enhanced Solid-State NMR of a ^{13}C-Labeled Signal Peptide Bound to Lipid-Reconstituted Sec Translocon. *J. Am. Chem. Soc.* **2011**, *133* (47), 19084−19086.
(40) Salnikov, E.; Ouari, O.; Koers, E.; Sarrouj, H.; Franks, T.; Rosay, M.; Pawsey, S.; Reiter, C.; Bandara, P.; Oschkinat, H.; et al. Developing DNP/Solid-State NMR Spectroscopy of Oriented Membranes. *Appl. Magn. Reson.* **2012**, *43* (1−2), 91−106.
(41) Hall, D. A.; Maus, D. C.; Gerfen, G. J.; Inati, S. J.; Becerra, L. R.; Dahlquist, F. W.; Griffin, R. G. Polarized-Enhanced NMR Spectroscopy of Biomolecules in Frozen Solution. *Science* **1997**, *276* (5314), 930−932.
(42) Rosay, M.; Zeri, A.-C.; Astrof, N. S.; Opella, S. J.; Herzfeld, J.; Griffin, R. G. Sensitivity-Enhanced NMR of Biological Solids: Dynamic Nuclear Polarization of Y21m Fd Bacteriophage and Purple Membrane. *J. Am. Chem. Soc.* **2001**, *123*, 1010−1011.
(43) Potapov, A.; Thurber, K. R.; Yau, W.-M.; Tycko, R. Dynamic Nuclear Polarization-Enhanced ^{1}H-^{13}C Double Resonance NMR in Static Samples Below 20 K. *J. Magn. Reson.* **2012**, *221*, 32−40.
(44) Salnikov, E.; Rosay, M.; Pawsey, S.; Ouari, O.; Tordo, P.; Bechinger, B. Solid-State NMR Spectroscopy of Oriented Membrane Polypeptides at 100 K with Signal Enhancement by Dynamic Nuclear Polarization. *J. Am. Chem. Soc.* **2010**, *132* (17), 5940−5941.

(45) Lesage, A.; Lelli, M.; Gajan, D.; Caporini, M. A.; Vitzthum, V.; Miéville, P.; Alauzun, J.; Roussey, A.; Thieuleux, C.; Mehdi, A.; et al. Surface Enhanced NMR Spectroscopy by Dynamic Nuclear Polarization. *J. Am. Chem. Soc.* **2010**, *132* (44), 15459−15461.
(46) Zagdoun, A.; Rossini, A. J.; Gajan, D.; Bourdolle, A.; Ouari, O.; Rosay, M.; Maas, W. E.; Tordo, P.; Lelli, M.; Emsley, L.; et al. Non-Aqueous Solvents for DNP Surface Enhanced NMR Spectroscopy. *Chem. Commun.* **2012**, *48* (5), 654−656.
(47) Rossini, A. J.; Zagdoun, A.; Lelli, M.; Canivet, J.; Aguado, S.; Ouari, O.; Tordo, P.; Rosay, M.; Maas, W. E.; Copéret, C.; et al. Dynamic Nuclear Polarization Enhanced Solid-State NMR Spectroscopy of Functionalized Metal−Organic Frameworks. *Angew. Chem., Int. Ed.* **2012**, *51* (1), 123−127.
(48) Vitzthum, V.; Mieville, P.; Carnevale, D.; Caporini, M. A.; Gajan, D.; Coperet, C.; Lelli, M.; Zagdoun, A.; Rossini, A. J.; Lesage, A. Dynamic Nuclear Polarization of Quadrupolar Nuclei using Cross Polarization from Protons: Surface-Enhanced Aluminium-27 NMR. *Chem. Commun.* **2012**, *48* (14), 1988−1990.
(49) Lee, D.; Takahashi, H.; Thankamony, A. S. L.; Dacquin, J. P.; Bardet, M.; Lafon, O.; De Paepe, G. Enhanced Solid-State NMR Correlation Spectroscopy of Quadrupolar Nuclei using Dynamic Nuclear Polarization. *J. Am. Chem. Soc.* **2012**, *134* (45), 18491−18494.
(50) Lafon, O.; Thankamony, A. S. L.; Kobayashi, T.; Carnevale, D.; Vitzthum, V.; Slowing, I. I.; Kandel, K.; Vezin, H.; Amoureux, J.-P.; Bodenhausen, G.; et al. Mesoporous Silica Nanoparticles Loaded with Surfactant: Low Temperature Magic Angle Spinning ^{13}C and ^{29}Si NMR Enhanced by Dynamic Nuclear Polarization. *J. Phys. Chem. C* **2012**, *117* (3), 1375−1382.
(51) van der Wel, P. C. A.; Hu, K. N.; Lewandowski, J.; Griffin, R. G. Dynamic Nuclear Polarization of Amyloidogenic Peptide Nanocrystals: GNNQQNY, a Core Segment of the Yeast Prion Protein Sup35p. *J. Am. Chem. Soc.* **2006**, *128* (33), 10840−10846.
(52) Rossini, A. J.; Zagdoun, A.; Hegner, F.; Schwarzwälder, M.; Gajan, D.; Copéret, C.; Lesage, A.; Emsley, L. Dynamic Nuclear Polarization NMR Spectroscopy of Microcrystalline Solids. *J. Am. Chem. Soc.* **2012**, *134* (40), 16899−16908.
(53) Gardiennet, C.; Schütz, A. K.; Hunkeler, A.; Kunert, B.; Terradot, L.; Böckmann, A.; Meier, B. H. A Sedimented Sample of a 59 kDa Dodecameric Helicase Yields High-Resolution Solid-State NMR Spectra. *Angew. Chem., Int. Ed.* **2012**, *51* (31), 7855−7858.
(54) Bertini, I.; Engelke, F.; Gonnelli, L.; Knott, B.; Luchinat, C.; Osen, D.; Ravera, E. On the Use of Ultracentrifugal Devices for Sedimented Solute NMR. *J. Biomol. NMR* **2012**, *54* (2), 123−127.
(55) Bertini, I.; Gallo, G.; Korsak, M.; Luchinat, C.; Mao, J.; Ravera, E. Formation Kinetics and Structural Features of Beta-Amyloid Aggregates by Sedimented Solute NMR. *ChemBioChem* **2013**, *14* (14), 1891−1897.
(56) Bertini, I.; Luchinat, C.; Parigi, G.; Ravera, E. Sednmr: On the Edge between Solution and Solid-State NMR. *Acc. Chem. Res.* **2013**, *46* (9), 2059−2069.
(57) Fragai, M.; Luchinat, C.; Parigi, G.; Ravera, E. Practical Considerations over Spectral Quality in Solid State NMR Spectroscopy of Soluble Proteins. *J. Biomol. NMR* **2013**, *57* (2), 155−166.
(58) Ravera, E.; Corzilius, B.; Michaelis, V. K.; Rosa, C.; Griffin, R. G.; Luchinat, C.; Bertini, I. Dynamic Nuclear Polarization in Sedimented Solutes. *J. Am. Chem. Soc.* **2013**, *135* (5), 1641−1644.
(59) Gelis, I.; Vitzthum, V.; Dhimole, N.; Caporini, M.; Schedlbauer, A.; Carnevale, D.; Connell, S.; Fucini, P.; Bodenhausen, G. Solid-State NMR Enhanced by Dynamic Nuclear Polarization as a Novel Tool for Ribosome Structural Biology. *J. Biomol. NMR* **2013**, *56* (2), 85−93.
(60) Barnes, A. B.; Mak-Jurkauskas, M. L.; Matsuki, Y.; Bajaj, V. S.; van der Wel, P. C. A.; DeRocher, R.; Bryant, J.; Sirigiri, J. R.; Temkin, R. J.; Lugtenburg, J.; et al. Cryogenic Sample Exchange NMR Probe for Magic Angle Spinning Dynamic Nuclear Polarization. *J. Magn. Reson.* **2009**, *198* (2), 261−270.
(61) Allen, P. J.; Creuzet, F.; Degroot, H. J. M.; Griffin, R. G. Apparatus for Low-Temperature Magic-Angle Spinning NMR. *J. Magn. Reson.* **1991**, *92* (3), 614−617.
(62) Pines, A.; Gibby, M. G.; Waugh, J. S. Proton-Enhanced Nuclear Induction Spectroscopy. A Method for High Resolution NMR of Dilute Spins in Solids. *J. Chem. Phys.* **1972**, *56* (4), 1776−1777.
(63) Bennett, A. E.; Rienstra, C. M.; Auger, M.; Lakshmi, K. V.; Griffin, R. G. Heteronuclear Decoupling in Rotating Solids. *J. Chem. Phys.* **1995**, *103* (16), 6951−6958.
(64) Goodman, D. S. The Interaction of Human Serum Albumin with Long-Chain Fatty Acid Anions. *J. Am. Chem. Soc.* **1958**, *80* (15), 3892−3898.
(65) Lange, S.; Linden, A. H.; Akbey, Ü.; Trent Franks, W.; Loening, N. M.; Rossum, B.-J. v.; Oschkinat, H. The Effect of Biradical Concentration on the Performance of DNP-MAS-NMR. *J. Magn. Reson.* **2012**, *216* (0), 209−212.
(66) Corzilius, B.; Andreas, L. B.; Smith, A. A.; Ni, Q. Z.; Griffin, R. G. Paramagnet Induced Signal Quenching in MAS-DNP Experiments in Frozen Homogeneous Solutions. *J. Magn. Reson.* **2014**, DOI: 10.1016/j.jmr.2013.11.013.
(67) Matsuki, Y.; Ueda, K.; Idehara, T.; Ikeda, R.; Kosuga, K.; Ogawa, I.; Nakamura, S.; Toda, M.; Anai, T.; Fujiwara, T. Application of Continuously Frequency-Tunable 0.4 THz Gyrotron to Dynamic Nuclear Polarization for 600 MHz Solid-State NMR. *J. Infrared, Millimeter, Terahertz Waves* **2012**, *33* (7), 745−755.
(68) Thiel, T. World's Highest Field NMR System for Dynamic Nuclear Polarization (DNP). http://www.bruker.com/news-records/single-view/article/bruker-successfully-installs-worlds-first-527-ghz-solid-state-dnp-nmr-system.html.
(69) Ni, Q. Z.; Daviso, E.; Can, T. V.; Markhasin, E.; Jawla, S. K.; Swager, T. M.; Temkin, R. J.; Herzfeld, J.; Griffin, R. G. High Frequency Dynamic Nuclear Polarization. *Acc. Chem. Res.* **2013**, *46* (9), 1933−1941, DOI: 10.1021/ar300348n.